Resistive wall mode stabilization by slow plasma rotation in DIII-D tokamak discharges with balanced neutral beam injection[a)]

E. J. Strait,[b)] A. M. Garofalo,[c)] G. L. Jackson, M. Okabayashi,[d)] H. Reimerdes,[c)] M. S. Chu, R. Fitzpatrick,[e)] R. J. Groebner, Y. In,[f)] R. J. LaHaye, M. J. Lanctot,[c)] Y. Q. Liu,[g)] G. A. Navratil,[c)] W. M. Solomon,[d)] H. Takahashi,[d)] and the DIII-D Team
General Atomics, P.O. Box 85608, San Diego, California 92186-5608

(Received 3 November 2006; accepted 9 January 2007; published online 22 March 2007)

Recent experiments in the DIII-D tokamak [J. L. Luxon, Nucl. Fusion **42**, 614 (2002)] show that the resistive wall mode (RWM) can be stabilized by smaller values of plasma rotation than previously reported. Stable discharges have been observed with beta up to 1.4 times the no-wall kink stability limit and ion rotation velocity (measured from CVI emission) less than 0.3% of the Alfvén speed at all integer rational surfaces, in contrast with previous DIII-D experiments that indicated critical values of 0.7%–2.5% of the local Alfvén speed. Preliminary stability calculations for these discharges, using ideal magnetohydrodynamics with a drift-kinetic dissipation model, are consistent with the new experimental results. A key feature of these experiments is that slow plasma rotation was achieved by reducing the neutral beam torque. Earlier experiments with strong neutral beam torque used "magnetic braking" by applied magnetic perturbations to slow the rotation, and resonant effects of these perturbations may have led to a larger effective rotation threshold. In addition, the edge rotation profile may have a critical role in determining the RWM stability of these low-torque plasmas. © *2007 American Institute of Physics*. [DOI: 10.1063/1.2472599]

I. INTRODUCTION

The long-wavelength ideal magnetohydrodynamic (MHD) kink mode often limits the stability of high-pressure magnetically confined plasmas, and the benefits of extending that limit with the stabilizing effect of a nearby conducting wall can be significant. In particular, "advanced" scenarios for steady-state tokamak fusion plasmas will require wall stabilization to achieve high fusion power density with reduced plasma current. In such configurations, wall stabilization can increase the kink mode pressure limit by as much as a factor of 2. In the presence of a real wall with finite conductivity, the kink mode is not fully stabilized, but is instead converted to a resistive wall mode (RWM) having a relatively slow growth rate of order τ_w^{-1}, where τ_w is the resistive decay time for induced currents in the wall. However, theoretical predictions have shown that full stabilization can be achieved either by direct feedback control (which is feasible because of the slow growth rate) or by rapid rotation of the plasma relative to the wall. An understanding of stabilization by plasma rotation is important in order to predict the stability of the RWM in future devices, and to assess the need for feedback control systems.

Recent DIII-D experiments have significantly reduced the upper bound on the rotation rate needed for RWM stabilization.[1] Previous experiments in DIII-D (Refs. 2–5) suggested that the critical rotation frequency, evaluated at the $q=2$ surface, was $\Omega_{\mathrm{crit}}\tau_A \sim 1\%-2\%$. [Here we define the Alfvén time as $\tau_A = R_0(\mu_0\rho_i)^{1/2}B_0^{-1}$, where R_0 is the major radius, B_0 is the toroidal field, and ρ_i the local mass density.] Similar values of $\Omega_{\mathrm{crit}}\tau_A$ have been observed in other experiments, including $\sim 1\%$ in JT-60U (Ref. 6) and $0.6\%-1.0\%$ in the Joint European Torus (JET).[7,8] A somewhat larger value of $\Omega_{\mathrm{crit}}\tau_A \sim 4\%-6\%$ at the $q=2$ surface in the National Spherical Torus Experiment (NSTX) (Refs. 8–10) is tentatively attributed to the larger fraction of trapped particles at low aspect ratio. In contrast to these previous results, recent DIII-D experiments have shown critical rotation values at the $q=2$ surface of $\Omega_{\mathrm{crit}}\tau_A \sim 0.3\%$.

An example with low critical rotation is shown in Fig. 1. In this discharge, the normalized beta is maintained at about 30% above the no-wall stability limit [Fig. 1(a)] as the rotation is slowly reduced [Fig. 1(c)]. { Here $\beta = \langle p \rangle 2\mu_0/B^2$ is the ratio of plasma pressure to magnetic field pressure, and the normalized beta is $\beta_N = \beta(aB/I)$ [%-m-T/MA], with a the minor radius of the plasma and I the plasma current.} The discharge remains stable until the rotation at the $q=2$ surface reaches about 15 km/s, corresponding to only $\Omega\tau_A \sim 0.3\%$ locally; at that time, a resistive wall mode grows [Fig. 1(a)].

Although initially surprising, the lower critical rotation observed in these experiments seems to be consistent with models of RWM stability. The key difference from previous experiments in DIII-D and in most other devices is that the rotation was reduced by decreasing the neutral beam torque [Fig. 1(b)], while minimizing the amplitude of nonaxisymmetric magnetic fields. As we will discuss in this paper, the capability to vary the neutral beam torque removed the need to use nonaxisymmetric fields in slowing the plasma rotation. In addition, the change in neutral beam torque can result in rather different forms of the rotation profile; hence, the value

[a)]Paper ZI1 6, Bull. Am. Phys. Soc. **51**, 337 (2006).
[b)]Invited speaker.
[c)]Also at: Columbia University, New York, New York.
[d)]Also at: Princeton Plasma Physics Laboratory, Princeton, New Jersey.
[e)]Also at: IFS, Univeristy of Texas, Austin, Texas.
[f)]Also at: FAR-TECH, Inc., San Diego, California.
[g)]Also at: Chalmers University of Technology, Göteborg, Sweden.

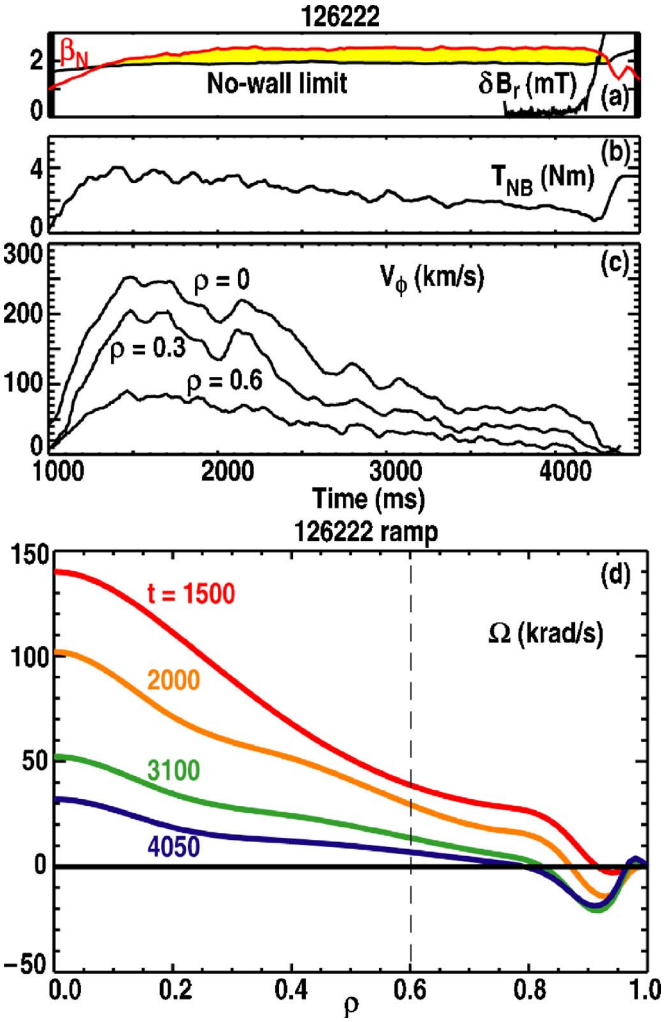

FIG. 1. (Color online) Time evolution of a discharge with diminishing neutral beam torque. [(a)–(c)] Time histories, including (a) normalized beta β_N, estimated no-wall stability limit, and amplitude δB_r of the nonrotating $n=1$ RWM; (b) neutral beam torque; and (c) toroidal rotation velocity at several values of normalized radius r/a. (d) Radial profiles of the measured rotation frequency at several times during the discharge.

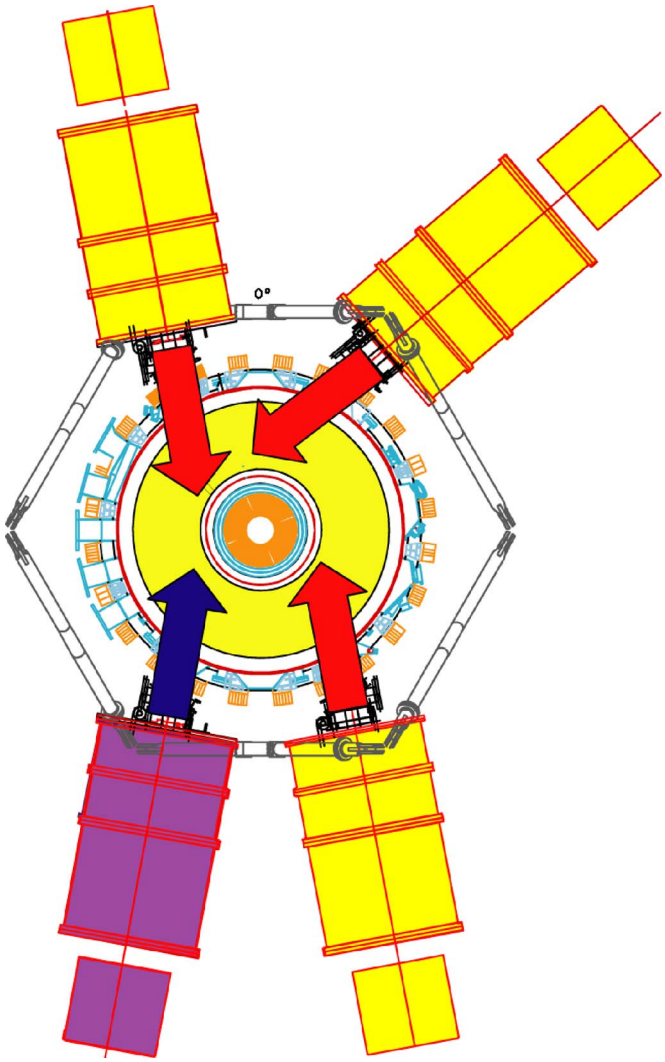

FIG. 2. (Color online) Plan view of the DIII-D tokamak, showing one beam line reoriented for counterinjection (clockwise), plus three neutral beam lines for co-injection (counterclockwise).

of the plasma rotation at a single radial location may not be sufficient to characterize the stability of the discharge. Similar low values of critical rotation have been observed in very recent JT-60U experiments[11] that also made use of reduced neutral beam torque and reduced magnetic field errors.

The remainder of the paper is organized as follows: Sec. II describes the experimental configuration and results. Section III discusses the relationship to earlier results and the role of magnetic braking. Section IV compares the new results to theoretical predictions of RWM stability limits. Conclusions are given in Sec. V, including the implications for RWM stability in future experiments.

II. EXPERIMENTAL CONFIGURATION AND RESULTS

The experiments described here were possible only with DIII-D's new capability of balanced neutral beam injection. The neutral beams used for heating all have a large tangential component, and until this year, all of the beams were aimed in the same direction. Therefore heating power was always accompanied by a strong torque, which drove high beta plasmas to typical central rotation speeds of 200–400 km/s. In 2006, one of the four beam lines was reoriented to the opposite toroidal direction (Fig. 2), allowing the capability of mixed co- and counterinjection relative to the plasma current direction.[12] This combination allows the injection of up to 10 MW with no net torque. The DIII-D plasma control system regulates the duty cycles of the co- and counter-beams, allowing the rotation to be controlled either by selecting the desired torque or by feedback control on the measured plasma rotation itself, while at the same time applying feedback control of the plasma beta. In the example shown in Fig. 1, the torque was programmed to decrease with time, from about 4 N m early in the discharge to 1.5 N m near the end. For comparison, the same heating power using pure co-injection would have applied 7–8 N m of torque. As is typical for DIII-D discharges, the reduction of rotation is accompanied by a mild reduction of energy confinement time (compensated by feedback control of the neutral beam power) and of angular momentum confinement; these changes may be a result of the reduction of $E\times B$ shear.[13]

Measurement of the toroidal rotation of the plasma, a crucial element of these experiments, is made with charge exchange recombination spectroscopy (CER) on the Doppler-shifted emission lines of carbon impurities. The results shown here incorporate recently developed corrections for atomic physics effects, including the energy dependence of the charge exchange cross section and contributions from excited beam neutrals.[14] In low-torque plasmas such as the case shown in Fig. 1, these corrections can be of the same order of magnitude as the measured rotation. However, the accuracy of the correction for the cross section energy dependence is improved by the fact that this diagnostic now views both co- and counterinjected neutral beams, in which the correction has opposite signs.

In these experiments, minimization of the $n=1$ component of the magnetic field was important as will be discussed later. A correction for the intrinsic error field (from sources such as nonaxisymmetry of the poloidal and toroidal field coil sets) was applied using either a 6-element set of coils external to the vacuum vessel (the "C-coil") or a 12-element set of coils inside the vessel (the "I-coil"). In most of the discharges discussed here, the error correction field was determined by an empirical algorithm based on the currents in the poloidal and toroidal field coils. In some discharges the algorithm was verified using dynamic error field correction, in which a feedback control system adjusts the error correction to minimize the $n=1$ response of the plasma. This technique exploits the resonant response of the stable resistive wall mode, which increases the sensitivity of the input measurement. However, the feedback control has a smoothing time constant that is long compared to the growth time of the RWM and, therefore, does not provide direct control of an unstable RWM. In 2006, one of the two current feed points for the toroidal field coil was rebuilt to reduce its error field;[12] as a result, the empirically determined $n=1$ correction field is now about 30% smaller.

The plasmas used in these experiments were designed to have a low stability limit to the $n=1$ kink mode,[3] so that it is easy to exceed the no-wall beta limit with the available heating power. They also have a broad current density profile with strong coupling to the wall, so that the wall-stabilized beta limit is significantly above the no-wall limit. Stability calculations with the DCON code[15] for recent discharges confirm previous calculations that the no-wall limit is well approximated by $\beta_N=(2.4\sim 2.6)l_i$, where l_i is the internal inductance. The ideal-wall limit in β_N is calculated to be about a factor of 1.6 larger.

The predicted value for the no-wall stability limit has been verified experimentally in several ways. In some experiments, balanced beam injection was used throughout the evolution of the discharge to create a plasma with near-zero rotation. As beta was raised under this condition of zero torque, the resistive wall mode appeared at the predicted no-wall stability limit.[1] In other experiments, an $n=1$ error field was applied in the middle of the discharge. It is now well known that when beta is above the no-wall limit, the RWM is only weakly damped by rotation and thus has a resonant response to external $n=1$ fields that results in strong braking of the plasma rotation.[16] This braking was seen as expected

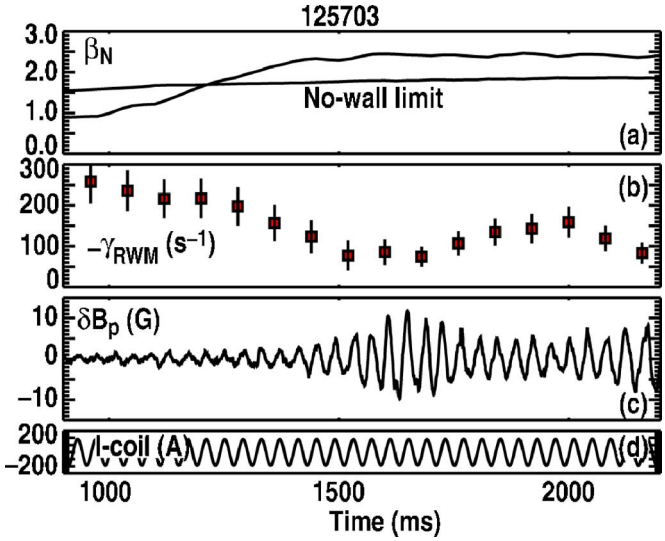

FIG. 3. (Color online) Time evolution of stability measurements with active MHD spectroscopy. (a) Normalized beta β_N and estimated no-wall stability limit; (b) measured damping rate $-\gamma$ of the RWM; (c) plasma response to an applied rotating $n=1$ perturbation; and (d) current in the perturbation coil (I-coil).

in the present discharges when beta was above the calculated no-wall stability limit, confirming the calculated limit to within 10%.[17] Finally, the same resonant response was measured continuously during the discharge as shown in Fig. 3. Here the internal control coils were used to apply a continuously rotating $n=1$ perturbation with a frequency of 25 Hz, near the natural frequency of the RWM [Fig. 3(d)], and the plasma response was measured with a pair of magnetic probes that has very little direct coupling to the coils. As beta rises above the no-wall stability limit [Fig. 3(a)], the measured response increases as expected [Fig. 3(c)], reaching amplitudes almost a factor of 10 larger than the low-beta response. In this technique known as "active MHD spectroscopy" the damping rate of the stable RWM resonance can be inferred from the amplitude and phase of the plasma response.[18] As seen in Fig. 3(b), the damping rate $(-\gamma)$ decreases rapidly from more than 250 s^{-1} to 70–80 s^{-1} when beta exceeds the no-wall stability limit, showing that stabilization by plasma rotation provides only weak damping of the RWM.

The critical rotation appears to have a definite threshold that increases weakly with beta. Figure 4 shows the time evolution of several different discharges, plotted as trajectories of beta and the rotation at $r/a=0.6$ (approximately the $q=2$ location). Here beta is normalized as the gain in beta over the no-wall limit: $C_\beta=[\beta-\beta(\text{no wall})]/[\beta(\text{ideal}-\text{wall})-\beta(\text{no}-\text{wall})]$, where the no-wall limit and ideal-wall limit are calculated with DCON for representative discharges. With this definition, $C_\beta=0$ represents beta at the no-wall limit, and $C_\beta=1$ represents beta at the ideal-wall limit. In the discharges shown in Fig. 4, beta was raised or held approximately constant while reducing the torque and plasma rotation. The discharges are stable with different paths through this space of rotation and beta, until the rotation decreases to about 10–20 km/s, at which point a resis-

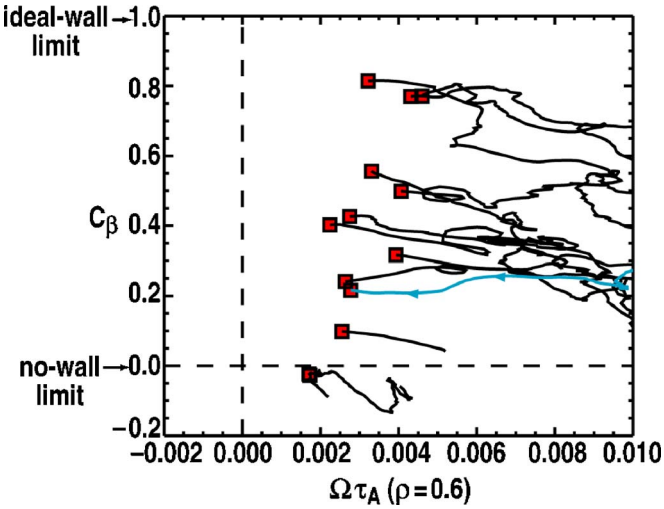

FIG. 4. (Color online) Trajectories of several discharges in beta and toroidal rotation, parameterized by time. The abscissa is the rotation frequency at radius $\rho \approx 0.6$, normalized by the local Alfvén time, and the ordinate is $C_\beta = [\beta - \beta(\text{no wall})]/[\beta(\text{ideal-wall}) - \beta(\text{no wall})]$. The square at the end of each trajectory represents the onset of a resistive wall mode.

tive wall mode grows. This threshold value is essentially independent of beta for C_β from 0.1 to 0.8.

Comparison of the rotation profiles indicates a well-defined threshold of rotation in the outer half of the plasma. Figure 5 shows the rotation profiles for a subset of the discharges of Fig. 4, at a time immediately before the onset of the RWM in each discharge. A representative q profile, determined from an equilibrium reconstruction using motional Stark effect measurements of the internal poloidal field, is also shown. Because of their different early time histories,

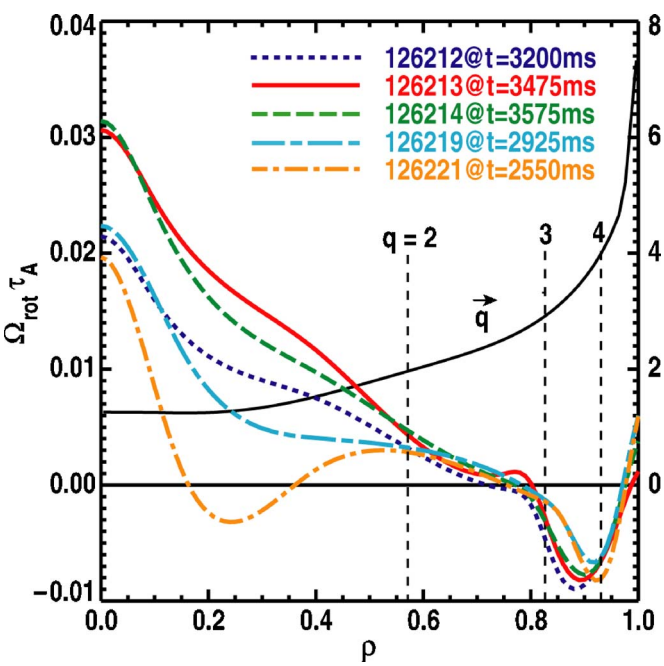

FIG. 5. (Color online) Measured profiles of toroidal rotation frequency (normalized by the Alfvén time) at the time of RWM onset, for several discharges from Fig. 4. A typical q profile and the radial locations of some integer rational surfaces are shown.

the central regions of the discharges have a wide variation in their rotation profiles at the RWM onset, suggesting that the central rotation has little impact on the RWM stability. The rotation profiles are remarkably similar in the outer portion of the discharge, from the $q=2$ surface outward ($r/a \geq 0.6$). This similarity suggests that rotation in this outer region is at the threshold for instability, but does not suggest whether one location within the region is more important than another. (The choice of $r/a=0.6$ in Fig. 4 and elsewhere was to provide a single representative rotation value from these profiles, and to allow comparison to earlier analysis where the rotation was also characterized by its value at the $q=2$ surface.) This question of where the damping occurs will be discussed further in Sec. IV.

III. MAGNETIC BRAKING AND TORQUE BALANCE

In previous experiments, measurements of RWM stability in DIII-D in the presence of a strong neutral beam torque required some form of "magnetic braking" to reduce the plasma rotation to the critical value. Two closely related braking methods were to reduce the current in the error correction coils, allowing the uncorrected part of the intrinsic error field to create a drag on the plasma rotation, or to apply an additional nonaxisymmetric field with the C-coil or I-coil set. Braking by applied fields with toroidal mode numbers $n=2$ and $n=3$ was found to be too weak to slow the plasma to the critical rotation for RWM stability, a result consistent with the drag expected from neoclassical toroidal viscosity.[19] Consequently, the earlier experiments usually used braking by fields that were resonant with the $n=1$ RWM: either reduced error correction (which had been designed to minimize the $n=1$ error field), or an additional applied $n=1$ field.

The resonant interaction of the applied field with the RWM leads to strong braking of the plasma rotation, since the nonaxisymmetric field is enhanced by the plasma's response. However, this feature also complicates the identification of the critical rotation for RWM stability. In the example shown in Fig. 6, the error correction coil current is ramped from 2 kA to zero between $t=2200$ and 2300 ms, and thus the resonant error field increases linearly during that time. The plasma response is measured by a midplane array of saddle loops, which are compensated to remove the direct coupling from the correction coil. The initial linear increase of the plasma response, proportional to the net error field, is accounted for as "resonant field amplification" by the weakly damped RWM;[16,20] and it is accompanied by a slow decrease of the plasma rotation. At about $t=2255$ ms, there is a distinct increase in the rate of change of the $n=1$ amplitude and of the rotation. This has been interpreted as the transition from resonant field amplification by a stable RWM to unstable growth of the RWM as the rotation threshold is crossed, in this case with a velocity of about 100 km/s at the $q=2$ surface, corresponding to $\Omega\tau_A \approx 2.0\%$.

A variation on this scenario offers a possible explanation why magnetic braking measurements may overestimate the critical rotation. As described above, the applied magnetic perturbation drives a resonant response by the stable RWM, and the amplified perturbation leads to slowing of the rota-

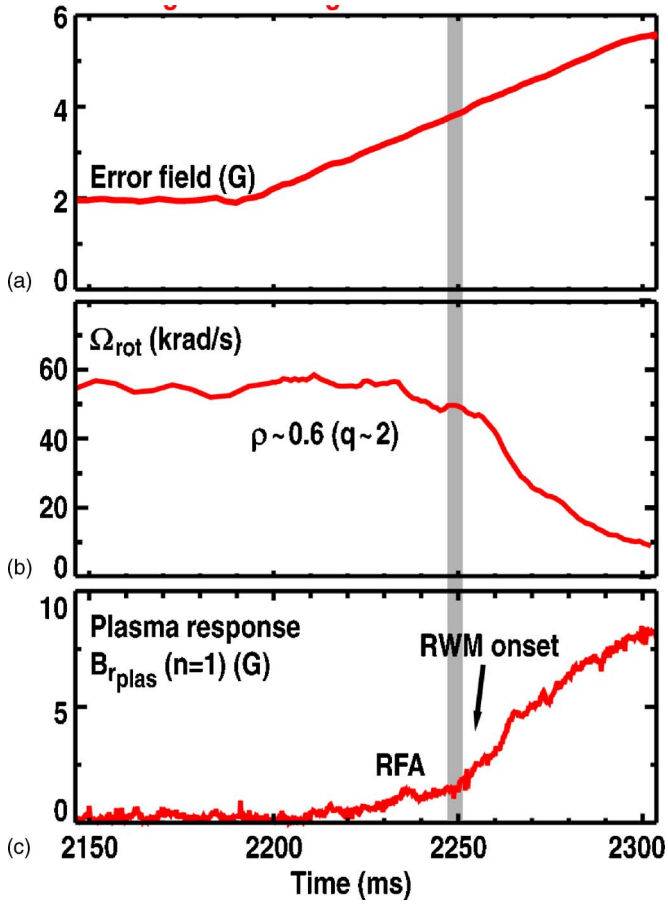

FIG. 6. (Color online) Time evolution of a discharge with strong magnetic braking. (a) Resonant error field; (b) toroidal rotation at $\rho \approx 0.6$; and (c) amplitude δB_r of the $n=1$ plasma response.

tion. However, the applied perturbation is also electromagnetically shielded by currents induced in the rotating plasma. As the rotation slows, the shielding effect is reduced, thus further increasing the amplitude of the plasma's resonant response. Under some conditions, this process can lead to a loss of the quasistationary balance between the neutral beam torque and the drag of the resonant perturbation, resulting in a rapid drop in rotation. That is, an instability of the rotation dynamics may occur before the MHD instability at $\Omega = \Omega_{crit}$ is encountered. This process is well known in the context of rotation locking and island growth driven by a resonant error field.[21] The dynamics of error fields, rotation locking, and resistive wall mode growth have also been studied for the case of the resistive wall tearing mode, in which island formation at a rational surface plays a key role.[22,23]

A simple RWM model has been developed[24] that includes ideal-MHD physics as well as rotation dynamics in the presence of an externally applied magnetic perturbation. It is a cylindrical model in which the resonant surface lies just outside the plasma, so no islands are formed. The RWM arises from a current-driven kink mode, and the dissipation required for rotational stabilization occurs in a thin inertial layer at the plasma edge. Therefore this model is not expected to provide realistic, quantitative predictions for DIII-D experiments, but it may capture the qualitative behavior. Although the model contains the full time-dependent dynamics of the RWM amplitude and plasma rotation, for simplicity we consider here only the stationary state in which all time derivatives are set to zero. This version of the model describes the torque balance equilibrium when the plasma is rotating at a constant rate and the RWM is stabilized by rotation.

The model yields an equation for the steady-state rotation frequency Ω in terms of the perturbed flux Ψ_c from the external coils or error field:

$$\nu_*(\Omega_0 - \Omega) - \nu_*\left(\frac{1-md}{1+md}\right)\left(\frac{(2md)^2\Omega}{[\Omega^2 + \kappa(1-md)]^2 + (\nu_*\Omega)^2}\right) \times |\Psi_c|^2 = 0.$$

The left-hand side of the equation is proportional to the total torque on the plasma which equals zero in a stationary state. The first term on the left, $\nu_*(\Omega_0 - \Omega)$, includes the driving torque from neutral beams or other sources, and angular momentum transport processes other than the drag due to the applied magnetic perturbation Ψ_c; when $\Psi_c = 0$ these contributions return the rotation to the unperturbed value Ω_0. The second term results from the drag due to Ψ_c. Both torque terms depend on the dissipation ν_* in the inertial layer. The RWM stability index κ runs from 0 at the no-wall limit to 1 at the ideal-wall limit, while m is the poloidal mode number and d is a coupling coefficient related to the radius of the wall.

This equation is evaluated with parameters representative of DIII-D plasmas.[24] The left-hand side, proportional to the net torque, is plotted in Fig. 7(a) for several values of the applied perturbation. Torque-balance equilibrium occurs where a curve crosses zero. With $\Psi_c = 0$, a stable torque-balance equilibrium exists at the unperturbed rotation $\Omega = \Omega_0$. At small but nonzero Ψ_c, the drag shifts the equilibrium point to smaller Ω. As Ψ_c increases, the torque curve becomes nonmonotonic and crosses zero in three places. These correspond to two stable equilibrium points at high and low rotation and an intermediate unstable equilibrium. As Ψ_c increases further, the two equilibria at larger rotation vanish, and the system must make a discontinuous jump to the low-rotation state in order to restore torque balance. If this new state has a rotation below the critical rotation Ω_{crit} for RWM stability, then the full dynamic solution would yield not a low-rotation torque balance equilibrium, but rather a low-rotation state with an unstable, growing RWM.

The equilibrium rotation frequency is plotted in Fig. 7(b) as a function of the applied perturbation Ψ_c, for several values of the initial, unperturbed rotation. Cases with a large initial rotation undergo the bifurcation described above at relatively large rotation. Cases with sufficiently small initial rotation do not undergo bifurcation, but evolve smoothly from higher to lower rotation as Ψ_c increases. We suggest that similar behavior may occur in DIII-D experiments: in cases with strong neutral beam torque and a large unperturbed rotation, where strong magnetic braking is used to reduce the rotation, the bifurcation of the torque balance could lead to a sudden decrease in rotation and increase in RWM amplitude that begins when the rotation is well above Ω_{crit}. On the other hand, cases with small neutral beam

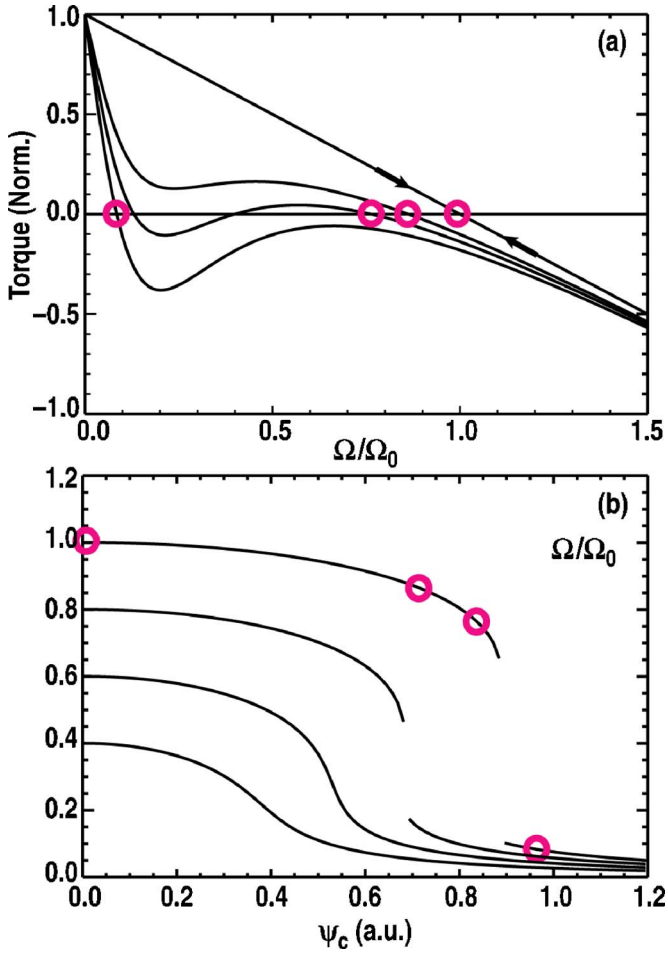

FIG. 7. (Color online) Torque balance calculated with the model of Ref. 24. (a) Net torque versus normalized plasma rotation Ω, for several values of magnetic perturbation Ψ_c. Circles indicate torque balance equilibrium for each condition. (b) Steady-state rotation Ω versus increasing Ψ_c, for several values of neutral beam torque. Circles indicate the same torque balance equilibria as in part (a). Some curves have a break where the rotation jumps to a lower branch. Portions of the curves that are inaccessible with increasing Ψ_c are not shown.

torque and little or no magnetic braking should be able to reach the expected MHD stability boundary at Ω_{crit}. An extension of this model now under development includes a more realistic dispersion relation for the RWM, and a neoclassical flow damping model[25] in place of the simple dissipation coefficient ν_*.

One implication of these results is to reinforce the importance of minimizing resonant field errors. A systematic study is still needed for the error field tolerance of high beta DIII-D plasmas with varying neutral beam torque. However, we note that even in the earlier experiments with strong neutral beam torque, an applied $n=1$ field with an estimated $m=2/n=1$ amplitude of 2–4 Gauss at the $q=2$ surface was sufficient to provide prompt braking of the rotation when beta was above the no-wall limit. This corresponds to a ratio $\delta B_r(2/1)/B_T=1-2\times10^{-4}$, above the ITER design maximum of 5×10^{-5} but of the same order of magnitude.

The onset of tearing modes represents an additional complication for understanding RWM stability in high beta, low rotation plasmas. In discharges where the torque is reduced at high beta (similar to the case in Fig. 1) $n=1$ tearing modes often appear as the plasma rotation approaches the minimum for the RWM stability. At the typical mode rotation frequencies of ≥1 kHz the wall provides the same stabilizing influence as an ideally conducting wall, yet the rotating modes are unstable; therefore, they are clearly distinct from resistive wall modes. Separate experiments in DIII-D and in JET indicate that the beta threshold for neoclassical tearing modes becomes smaller as the plasma rotation is reduced.[26,27] A correlation between tearing mode onset and the RWM threshold may be explained by a rapid increase of the tearing stability index Δ' near an ideal MHD stability boundary.[28]

IV. COMPARISON TO STABILITY MODELING

The resistive wall mode stability in these experiments has been modeled using MARS-F,[29] a linear MHD stability code that includes a resistive wall and toroidal rotation of the plasma. MARS-F employs a plasma model without resistivity, but includes two models for the ion Landau damping that is believed to be important in the stabilization of the RWM.[30] In the "sound wave" model the damping is modeled as a parallel viscosity, approximated as the cylindrical plasma viscosity multiplied by a coefficient $\kappa_\parallel$, which is treated as an adjustable parameter. The "kinetic damping" model is based on drift-kinetic analysis[31] and has no free parameters.

Stability modeling was based on a stable experimental case with beta midway between the no-wall and ideal-wall limits ($C_\beta\approx0.5$), and a rotation frequency at the $q=2$ surface of less than 10 krad/s. The experimental equilibrium was reconstructed by fitting to external magnetic data, measured pressure profile data (ion temperature from charge exchange recombination spectroscopy, electron temperature from Thomson scattering, and electron density from Thomson scattering and interferometer measurements) and the internal magnetic field pitch from motional Stark effect measurements. This equilibrium and the measured toroidal rotation profile were used as an input to MARS-F, and the critical rotation for RWM stability was determined by scaling the rotation profile. The critical rotation frequency predicted with the sound wave damping model was significantly larger than the experimental rotation.[1] However, the critical rotation frequency with the kinetic damping model was found to be about 0.7 of the experimental value, consistent with the observation that this discharge was stable.

The critical rotation calculated by MARS-F with the kinetic damping model is in reasonable agreement with the measured values, as shown in Fig. 8(a), and reproduces the weak increase with C_β. The experimentally determined critical rotation for the 2006 experiments with low neutral beam torque is a factor of 2–10 below the earlier results with magnetic braking, also shown in Fig. 8(a). The measured rotation profile of the stable, low-torque case used for the stability calculations is shown in Fig. 8(b); the rotation frequency is under 20 krad/s everywhere in the plasma. In contrast, the rotation profile at the RWM onset in a case with magnetic braking [also shown in Fig. 8(b)] is much larger.

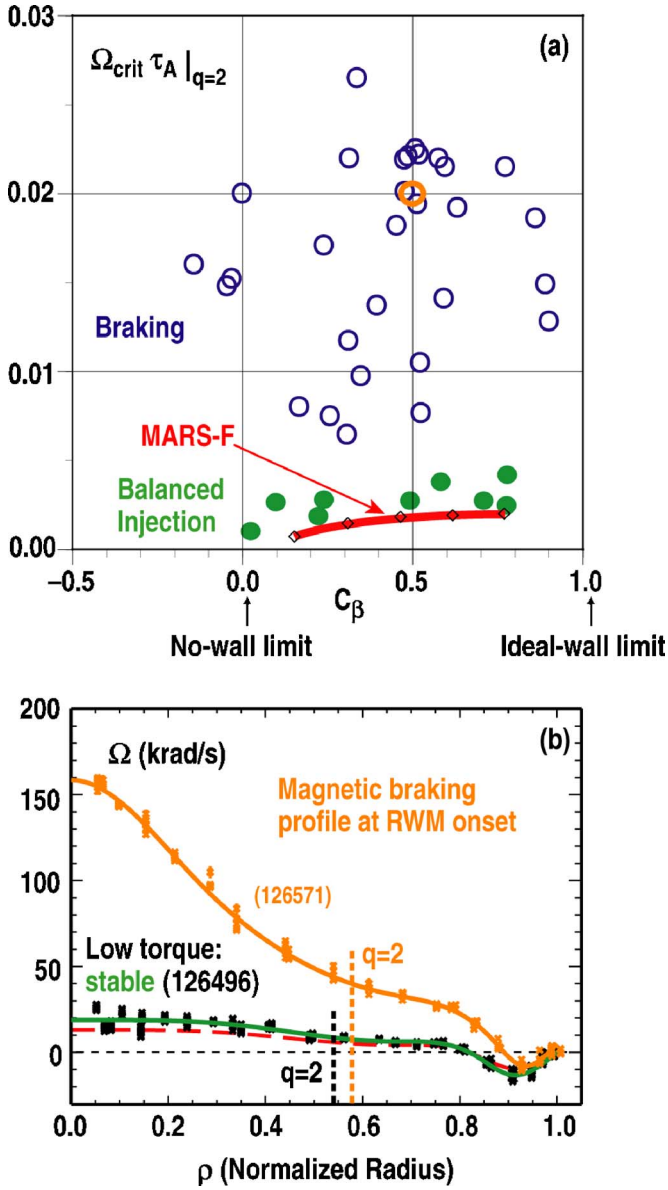

FIG. 8. (Color online) (a) Recent measurements of critical rotation Ω_{crit} with reduced neutral beam torque (closed symbols) compared to the corresponding critical rotation calculated with MARS-F (horizontal curve) and to earlier measurements of critical rotation with magnetic braking (open symbols). The abscissa is C_β and the ordinate is $\Omega_{crit}\ \tau_A$. (b) Rotation frequency profiles for the stable, low-torque case used in the MARS-F calculation (lower solid curve), and a high-torque case with strong magnetic braking (upper solid curve). The high-torque profile represents the time of the RWM onset. The rotation profile calculated by MARS-F to be marginally stable is also shown (dashed curve).

In previous comparisons to magnetic braking experiments,[4,5,8] the critical rotation predicted with the kinetic damping model was consistently below the experimental value, as might be expected if the magnetic braking technique overestimates the critical rotation. However, the predicted critical rotation shown in Fig. 8 for the recent experiments is significantly smaller than the earlier predictions associated with the braking experiments. As discussed next, the reason for this difference is likely to be a difference in the rotation profiles.

The additional stability in the recent MARS-F predictions may be a result of a significant negative rotation near the edge, which can be seen in Fig. 8(b) and also in Fig. 1(b). The earlier results with unidirectional beam injection had little or no negative edge rotation. However, in the present case with nearly balanced beam injection, the absolute value of the measured rotation at the $q=4$ surface has become comparable to or larger than the rotation at the $q=2$ surface. With slow rotation, the RWM damping is expected to be localized near the resonant surfaces.[30] Furthermore, the threshold rotation frequency for strong local damping is estimated to vary as $1/q^2$.[31] These trends suggest that the rotation profile of Fig. 8(b) might result in a strong contribution to RWM damping by the $q=4$ surface, and indeed MARS-F predicts a negative toroidal rotation for the RWM, consistent with a strong coupling to the region of negative plasma rotation. Furthermore, in most low-rotation cases, the RWM is experimentally observed to rotate in the negative (counterinjection) direction as it becomes unstable.

Although the measured critical rotation seems to be in reasonable agreement with theoretical modeling, any quantitative comparisons must be viewed cautiously, since neoclassical effects and related issues of poloidal rotation create some uncertainty in both the measurements and the models. The measured toroidal rotation rates shown here are those of carbon impurity ions, not the main deuterium ions. The difference in toroidal rotation between carbon and deuterium can be calculated if their poloidal rotation is known.[32] Since the deuterium rotation cannot be readily measured, a calculation with the NCLASS code[33] uses neoclassical theory to determine the poloidal rotation velocities and yields a difference of 10–20 krad/s between the toroidal rotation frequencies of carbon and deuterium ions in one of the present discharges. This correction is comparable to the measured carbon rotation frequency in these low-torque cases. However, recent experiments[14] show significant discrepancies between neoclassical predictions and experimental measurements of the poloidal rotation of impurity ions, suggesting that there may be sources of poloidal rotation that are not accounted for in the neoclassical model. This discrepancy creates uncertainty in estimating the deuterium rotation from measurements of carbon rotation. Furthermore, present theories of RWM stability are based on toroidal rotation only; the effects of nonzero poloidal flow on RWM stability are unknown.

V. DISCUSSION AND CONCLUSIONS

Recent DIII-D experiments have shown that the resistive wall mode is stabilized at relatively modest values of neutral beam torque and plasma rotation, with toroidal rotation frequencies on the order of $\Omega_{crit}\tau_A \sim 0.3\%$ at the $q=2$ surface. These values are a factor of 2–10 below previously reported values of critical rotation in DIII-D. The two key operational features in obtaining this new result were the reduction of plasma rotation by varying the neutral beam torque and minimization of nonaxisymmetric magnetic fields.

Stability with rotation just above the critical value has been sustained for up to 1 s. In the example shown in Fig. 9, RWM stability is maintained in conditions of nearly bal-

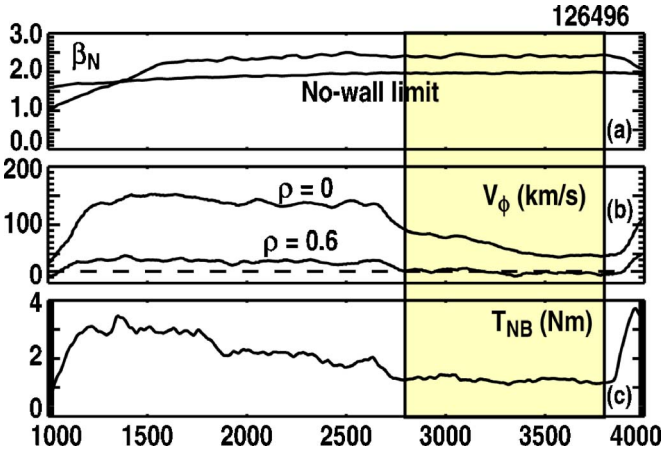

FIG. 9. (Color online) Time evolution of a stable discharge with low neutral beam torque and low rotation, including (a) normalized beta β_N and estimated no-wall stability limit; (b) toroidal rotation velocity V_ϕ at several values of normalized radius r/a; and (c) neutral beam torque T_{NB}. The region between vertical lines indicates a 1-s interval with $T_{\mathrm{NB}} \leq 1.3$ N m and $\Omega_{\mathrm{crit}}\ \tau_A \leq 0.5\%$ ($V_\phi \leq 20$ km/s) at $\rho=0.6$.

anced beam injection, with only 10%–15% of the torque that would have been applied by co-injected beams at the same heating power. During this interval, the rotation in the outer region of the plasma ($\rho \geq 0.6$) and at all integer rational surfaces ($q \geq 2$) is maintained near the critical value, with $\Omega \tau_A \leq 0.5\%$. The stable interval with low rotation is much longer than the resistive wall time ($\sim$3 ms for the $n=1$ RWM) or the momentum confinement time (on the order of 100 ms).

These experimental results are consistent with preliminary stability calculations using the kinetic damping model in MARS-F. The stable, low-rotation discharge of Fig. 9 was the basis for the stability analysis shown earlier in Fig. 8, where the critical rotation was calculated to be about 0.7 times the experimental rotation. There are at least two possible reasons for the lower critical rotation relative to previous results in both experiment and modeling: differences in rotation dynamics at high and low beam torque, and differences in the shape of the rotation profile at high and low beam torque.

A simple model of the rotation dynamics suggests that, with the large neutral beam torque typical of previous experiments with co-injected beams, the resonant magnetic braking required to slow the plasma rotation can lead to a bifurcation of the torque-balance equilibrium at rotations above the RWM critical value. This effective RWM threshold determined by the rotation dynamics represents the operating limit in high-torque plasmas with magnetic braking, but overestimates the threshold that would be found at low torque. More realistic modeling of this process is needed, including the radial distribution of applied torque and radial transport of momentum.

The rotation profile becomes significantly different in shape as the torque is reduced, with negative rotation developing near the edge as the positive core rotation decreases. This negative rotation could have a significant stabilizing effect, owing to the stronger damping effect expected at large values of q. Neoclassical calculations predict that the deuterium rotation should be larger than the measured carbon rotation and perhaps even positive at the edge. However, the poloidal rotation model in the neoclassical calculation may not be complete. An improved understanding of poloidal rotation is needed in order to reliably estimate the toroidal rotation profile of the deuterium ions.

Poloidal rotation physics may also need to be added to theories of RWM stability. Present RWM models assume no poloidal rotation. However, as the toroidal rotation becomes small, the poloidal rotation may become more important, particularly in light of measurements that indicate poloidal rotation speeds larger than predicted by neoclassical theory.

These results are encouraging for the prospects of rotational stabilization of the RWM in ITER. They seem to provide a successful benchmark of the kinetic damping model, and the same model predicts that the rotation in ITER's advanced scenario will be near the critical value.[34] Indeed, the critical rotation in the DIII-D experiments of $\Omega_{\mathrm{crit}}\tau_A \sim 0.3\%$ at $r/a=0.6$ is comparable to the value of $\Omega\tau_A$ predicted in ITER at the same location.[35] However, there is significant uncertainty in extrapolating these results to ITER. As discussed above, the correction to obtain the deuterium ion rotation in DIII-D is not well known and could be of the same order as the measured carbon rotation. Furthermore, the transport of angular momentum is not well understood, and so there is uncertainty in the predicted rotation profile for ITER. Finally, other perturbations such as edge-localized modes (ELMs) may transiently reduce the rotation and destabilize an RWM,[36] and therefore active feedback stabilization is likely to be needed in addition to rotational stabilization. Further experiments and modeling in these areas are needed.

The DIII-D results also imply that there is an upper limit on the resonant error field amplitude that can be tolerated in plasmas where the RWM is stabilized by rotation. Experiments in JET (Ref. 37) as well as DIII-D have indicated that $m=2/n=1$ error fields must be kept below $\delta B_r(2/1)/B_T=1-2\times10^{-4}$ in order to avoid strong braking of the rotation when beta is above the no-wall limit. However, at low neutral beam torque, the tolerance of error fields is likely to decrease. Systematic experiments are needed to quantify error field effects as the neutral beam torque is varied.

Future DIII-D experiments will continue to use variable neutral beam torque to study RWM stability, angular momentum transport, and the interaction of error fields with plasma rotation and plasma stability. The low-rotation plasmas will also provide an environment for tests of active feedback control of the RWM.

ACKNOWLEDGMENTS

This work was supported by the U.S. Department of Energy under Contract Nos. DE-FC02-04ER54698, DE-FG02-89ER53297, DE-AC02-76CH03073, DE-FG03-97ER54415, and DE-FG03-99ER52791.

[1] H. Reimerdes, A. M. Garofalo, G. L. Jackson *et al.*, Phys. Rev. Lett. **98**, 055001 (2007).
[2] E. J. Strait, T. S. Taylor, A. D. Turnbull, J. R. Ferron, L. L. Lao, B. Rice,

O. Sauter, S. J. Thompson, and D. Wroblewski, Phys. Rev. Lett. **74**, 2483 (1995).
[3] A. M. Garofalo, A. D. Turnbull, M. E. Austin *et al.*, Phys. Rev. Lett. **82**, 3811 (1999).
[4] R. J. La Haye, A. Bondeson, M. S. Chu, A. M. Garofalo, Y. Q. Liu, G. A. Navratil, M. Okabayashi, H. Reimerdes, and E. J. Strait, Nucl. Fusion **44**, 1197 (2004).
[5] H. Reimerdes, J. Bialek, M. S. Chance *et al.*, Nucl. Fusion **45**, 368 (2005).
[6] S. Takeji, S. Tokuda, T. Fujita *et al.*, Nucl. Fusion **42**, 5 (2002).
[7] T. C. Hender, M. Gryaznevich, Y. Q. Liu, *et al.*, in *Proceedings of the 20th IAEA Fusion Energy Conference 2004*, Vilamoura, Portugal (IAEA, Vienna, 2004), Paper No. EX/P2-22.
[8] H. Reimerdes, T. C. Hender, S. A. Sabbagh *et al.*, Phys. Plasmas **13**, 056107 (2006).
[9] A. C. Sontag, S. A. Sabbagh, W. Zhu *et al.*, Phys. Plasmas **12**, 056112 (2005).
[10] S. A. Sabbagh, A. C. Sontag, J. M. Bialek *et al.*, Nucl. Fusion **46**, 635 (2006).
[11] M. Takechi, G. Matsunaga, N. Aiba *et al.*, Phys. Rev. Lett. **98**, 055002 (2007).
[12] A. G. Kellman, "System upgrades to the DIII-D facility," in *Proceedings of the 24th Symposium on Fusion Technology 2006*, Warsaw, Poland (to be published).
[13] P. A. Politzer, C. C. Petty, R. J. Jayakumar *et al.*, in *Proceedings of the 21st IAEA Fusion Energy Conference 2006*, Chengdu, China (IAEA, Vienna, 2006), Paper No. EX/P1-9.
[14] W. M. Solomon, K. H. Burrell, R. Andre, L. R. Baylor, R. Budny, P. Gohil, R. J. Groebner, C. T. Holcomb, W. A. Houlberg, and M. R. Wade, Phys. Plasmas **13**, 056116 (2006).
[15] A. H. Glasser and M. S. Chance, Bull. Am. Phys. Soc. **42**, 1848 (1997).
[16] A. M. Garofalo, T. H. Jensen, L. C. Johnson *et al.*, Phys. Plasmas **9**, 1997 (2002).
[17] A. M. Garofalo, M. S. Chu, E. J. Doyle *et al.*, in *Proceedings of the 21st IAEA Fusion Energy Conference 2006*, Chengdu, China (IAEA, Vienna, 2006), Paper No. EX/7-1Ra.
[18] H. Reimerdes, M. S. Chu, A. M. Garofalo, G. L. Jackson, R. J. La Haye, G. A. Navratil, M. Okabayashi, J. T. Scoville, and E. J. Strait, Phys. Rev. Lett. **93**, 135002 (2004).
[19] G. L. Jackson, J. M. Bialek, A. M. Garofalo *et al.*, in *Proceedings of the 33rd EPS Conference on Plasma Physics 2006*, Rome, Italy, Europhysics Conference Abstracts (EPS, Paris, 2006), Vol. 30I, Paper No. P-5.143.
[20] A. H. Boozer, Phys. Rev. Lett. **86**, 5059 (2001).
[21] R. Fitzpatrick, Phys. Plasmas **5**, 3325 (1998).
[22] C. G. Gimblett and R. J. Hastie, Phys. Plasmas **11**, 1019 (2004).
[23] C. G. Gimblett and R. J. Hastie, Phys. Plasmas **7**, 258 (2000).
[24] R. Fitzpatrick, Phys. Plasmas **9**, 3459 (2002).
[25] K. C. Shaing, Phys. Plasmas **11**, 5525 (2004).
[26] R. Buttery, Bull. Am. Phys. Soc. **51**, 141 (2006).
[27] T. C. Luce K. H. Burrell, R. J. Buttery *et al.*, "Dependence of confinement and stability on variations in the external torque in the DIII-D tokamak," in *Proceedings of the 21st IAEA Fusion Energy Conference 2006*, Chengdu, China (IAEA, Vienna, 2006), Paper No. PD-3.
[28] D. P. Brennan, R. J. La Haye, A. D. Turnbull *et al.*, Phys. Plasmas **10**, 1643 (2003).
[29] Y. Q. Liu, A. Bondeson, C. M. Fransson, B. Lennartson, and C. Breitholtz, Phys. Plasmas **7**, 3681 (2000).
[30] Y. Liu, A. Bondeson, M. S. Chu *et al.*, Nucl. Fusion **45**, 1131 (2005).
[31] A. Bondeson and M. S. Chu, Phys. Plasmas **3**, 3013 (1996).
[32] L. R. Baylor, K. H. Burrell, R. J. Groebner, W. A. Houlberg, D. P. Ernst, M. Murakami, and M. R. Wade, Phys. Plasmas **11**, 3100 (2004).
[33] W. A. Houlberg, K. C. Shaing, S. P. Hirshman, and M. C. Zarnstorff, Phys. Plasmas **4**, 3230 (1997).
[34] Y. Liu, A. Bondeson, Y. Gribov, and A. Polevoi, Nucl. Fusion **44**, 232 (2004).
[35] A. R. Polevoi, S. Yu. Medvedev, V. D. Pustovitov, V. S. Mukhovatov, M. Shimada, A. A. Ivanov, Yu. Yu. Poshekhonov, and M. S. Chu, in *Proceedings of the 19th IAEA Fusion Energy Conference 2002*, Lyon, France (IAEA, Vienna, 2006), Paper No. CT/P-08.
[36] A. M. Garofalo, E. J. Doyle, J. R. Ferron *et al.*, Phys. Plasmas **13**, 056110 (2006).
[37] T. C. Hender, H. Reimerdes, M. S. Chu *et al.*, in *Proceedings of the 21st IAEA Fusion Energy Conference 2006*, Chengdu, China (IAEA, Vienna, 2006), Paper No. EX/P8-18.